Comparing dithered and encoded shooting for Exploration nodal surveys

Introduction

Source vessels involved in Ocean Bottom Node (OBN) data acquisition use airgun sources, which fire in a dithered manner to facilitate deblending of the data. The number of sources per vessel varies depending on the objective of the survey. For Development surveys with a 4D objective, one usually aims at avoiding self-blending in the reservoir zone. Sampling and free record length requirements then typically restrict the number of sources per vessel to two or three. For Exploration OBN surveys self-blending is traditionally considered less of an issue, as one typically aims at structural imaging. Nevertheless, the maximum number of sources per vessel involved in such surveys is four at the moment, because of the increasing difficulty of deblending with higher blending fold.

Encoded shooting, in which firing delays between sources are deterministic rather than random, may offer a way forward in terms of using more sources per vessel, provided we can demonstrate that data quality after decoding is on par or better than after deblending. In this paper we focus on the case of Exploration OBN surveys and compare dithered shooting with four airguns against encoded shooting with 6 airguns. The comparison is made on Signal to Noise Ratio (SNR) in the data domain, low frequency Reverse Time Migration (RTM) images and ultra-low frequency Full Waveform Inversion (FWI) velocity updates.

Dithered versus Apparition encoded shooting

Simultaneous source acquisitions are conducted by applying random delays to source firing times. Originally, the randomness in source firing times was exploited by using noise reduction methods to deblend the data. Nowadays, this is typically achieved by solving inverse problems with sparsity constraints (Abma and Foster, 2020, Kumar, et al., 2020; JafarGandomi, et al., 2021).

Seismic Apparition is a technique for conducting simultaneous source seismic surveys in which multiple sources are fired at approximately the same time with small (up to 200 ms) deterministic relative delays between them. Apparition decoding is also based on solving inverse problems. It has been shown (Andersson et al., 2017, Amundsen et al., 2018) that decoding can be performed exactly in the FK-domain for low temporal and spatial frequencies. This can be used to set up inversion schemes for decoding in other domains.

Apparition encoded shooting has several advantages in terms of data quality. First, the small encoding delays ensure that strong events in a salvo of N encoded shots (like the direct arrival) overlap with strong ones, and weak events (like reservoir reflections) with weak ones. This strong-on-strong, weak-on-weak property holds until the next salvo of N encoded shots is fired. It makes the inverse problem of decoding the N shots in the salvo well-posed. In contrast, dithered shooting leads to strong events overlapping with weak events. For the case of OBN data, the difference between a direct arrival and a deep reservoir reflection can be easily 40 dB. Small imperfections in the estimation of the direct arrival can therefore have a significant impact on the recovery of these weak reflections during deblending.

The second advantage is that low frequencies in a salvo of N encoded shots with small relative delays stack up in phase. Ambient noise is measured only once during such a salvo, so the SNR in encoded data goes up by a factor of N. In decoding, both signal and ambient noise in the encoded data are divided over the decoded shots. Low frequency SNR on decoded shots goes up by a factor $\sqrt{N}$ consequently. Apart from this effect, the inverse problems solved in deblending and decoding each have intrinsic noise penalization, which can only be compared through field tests.

The field test

We have conducted a field test of hexa-source Apparition encoded shooting during a production OBN survey. Both production and test data were shot with the Gemini low frequency enhanced source

(Udengaard, 2023). The Apparition test comprised six hexa-source sail lines. The sources were 60 m apart in the crossline direction, Apparition encoded salvos of 6 encoded shots were fired at 60 m inline increments. The sail lines were roughly 60 km long. The test data therefore consists of a narrow source swath of 2.1 by 60 km sampled on a regular 60 by 60 m grid. The production data were shot with four sources firing in a dithered manner on a staggered 100 by 50 m grid. For the comparison in this abstract, we have extracted six sail lines of production data, which covered approximately the same area as the test data (2.3 by 60 km). To compare these data while the production survey was still ongoing, 19 ocean bottom test nodes were co-located with production nodes along a sail line and retrieved ahead of the production nodes. Spacing between these nodes was 1,200 m.

Compressor capacity of the source vessel only allowed for a firing pressure of 1,500 psi for the hexa-source test lines, as opposed to the standard 2,000 psi during the quad source production lines. Since the spectral output below the resonance frequency of the airgun scales as $p^{4/3}f^2$ (Baeten et al, 2021), the SNR of the Apparition encoded data should reduce by a factor of ~0.7 for these frequencies.

On theoretical grounds, the difference in source sampling between production and test data should lead to a factor of $\sqrt{100 \times 50}/60 \approx 1.2$ improvement of SNR in RTM images or FWI gradients based on Apparition decoded data compared to production data. At low frequencies, there is the additional factor $\sqrt{6}$ explained in the previous section. Below the resonance frequency of the airgun, the net SNR improvement in RTM images or FWI gradients should therefore be $0.7 \times 1.2 \times \sqrt{6} \approx 2$, showing that there is ample room to go to wider hexa-source tows while retaining good SNR.

Deblending and decoding results

The six quad-source dithered sail lines and the six hexa-source Apparition encoded sail lines were deblended and decoded, respectively. The results were subsequently filtered into two low frequency bands by applying Ormsby filters with corner frequencies 0-0-1-2 Hz and 0-0-2-4 Hz. The results are shown in Figure 1. Deblended data are in the top row, decoded data in the bottom one. The rightmost column contains the full bandwidth data.

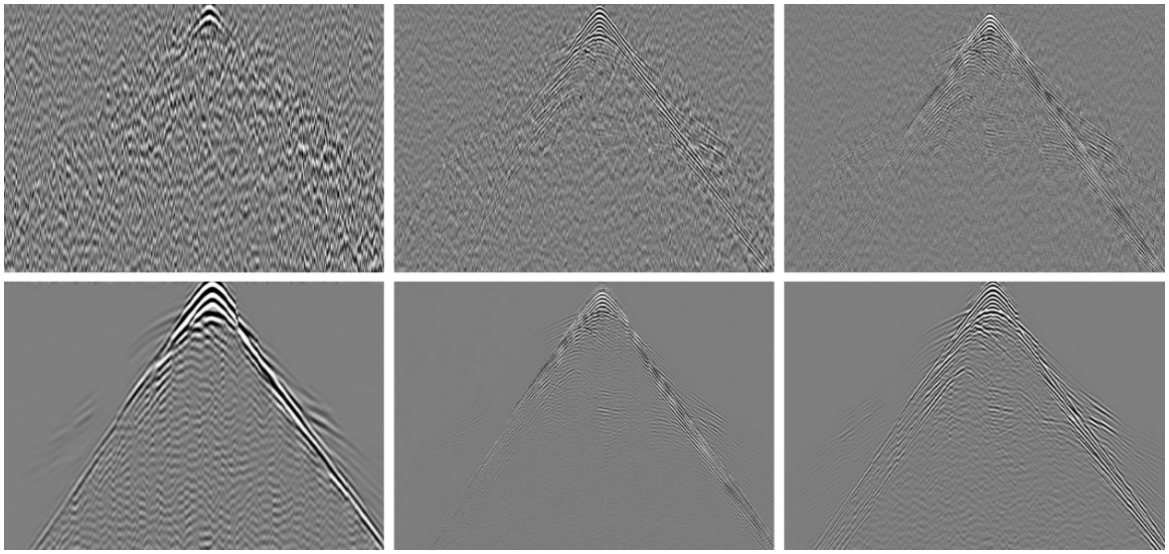

Figure 1 *Comparison of deblended (top row) and decoded (bottom row) OBN gathers, band passed by a 0-0-1-2 Hz Ormsby filter (left column), a 0-0-2-4 Hz Ormsby filter (middle column) and at full bandwidth (right column). Horizontal axis spans roughly 60 km, vertical axis spans 20 seconds.*

The SNR on the Apparition decoded data is clearly superior, both for the low frequencies *and* over the full bandwidth. The latter suggests that the inverse problem for decoding leads to better solutions than the one for deblending and/or that ambient noise rejection in decoding is more effective than in

deblending. It should be mentioned, however, that the background noise level at very low frequencies was higher during the production shooting than during the Apparition test, which may partially explain the difference between deblending and decoding in the 0-0-1-2 Hz band.

Migration test

The deblended quad source production data and the decoded hexa-source, as recorded by the 19 test nodes at 1,200 m spacing, were subsequently imaged by RTM. We used an existing velocity model, which has been derived from towed streamer WAZ data acquired in the survey area. Figure 2 shows a comparison of 12 Hz RTM images. Minimal preprocessing in the form of zero phasing and debubble has been applied to both data sets. The image of the deblended production data is on the left, the image of the decoded Apparition data on the right. The image of the full towed streamer WAZ data is shown in the middle as a reference. It is obvious that the combination of a single line of 19 nodes spaced at 1,200 m and a 2.3 km (for the deblended data) or 2.1 km (for the decoded data) by 60 km source swath has quite limited illumination properties. The main conclusion from this test is that the image of the decoded Apparition data is on par with the image of the deblended production data.

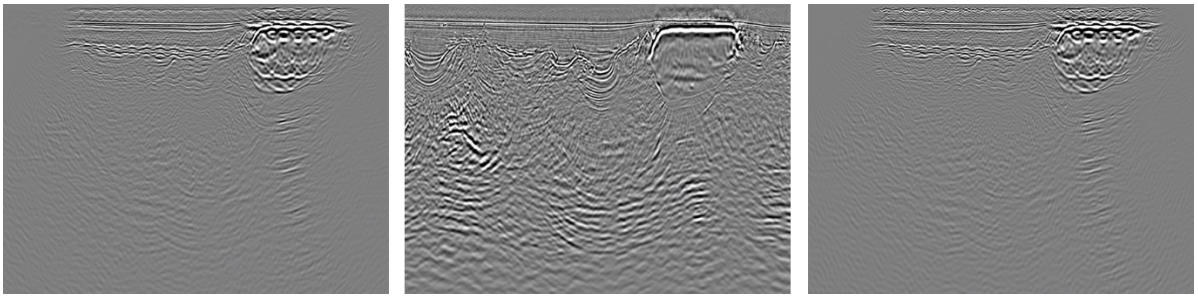

Figure 2 *Comparison of RTM images along the node line. Left: image of deblended production data, middle: image of towed streamer WAZ data, right: image of decoded Apparition data. Horizontal axis spans roughly 20 km, vertical axis roughly 15 km.*

FWI test

Finally, we compare the production and test data of the 19 nodes on FWI performance by an ultra-low frequency FWI test. The results are shown in Figure 3. The top left picture in that Figure is the towed streamer derived velocity model, the top right one is a uniform 3% perturbation of that model. In each picture, two dashed lines have been added for ease of interpretation. The one in the top right corner of each picture shows the contours of a salt body, the other marks a gradient in the velocity model.

We ran 6 iterations of elastic FWI on data band passed with a zero-phase filter with corner frequencies 0.2, 0.5, 0.6, and 1.6 Hz, using the perturbed model as starting model. The slightly smoothed FWI velocity update for deblended production data is in the bottom left, the slightly smoothed FWI velocity update for Apparition decoded data in the bottom right. The latter is a better approximation of the actual velocity perturbation, because the red parts are more uniform. Given the data domain comparison in Figure 1, which shows clear diving waves for the decoded Apparition data in the lowest frequency band, this should not come as a surprise. We remark that the velocity model derived from towed streamer WAZ data will in general not be fully correct, so the FWI velocity updates do not have to completely agree with the velocity perturbation.

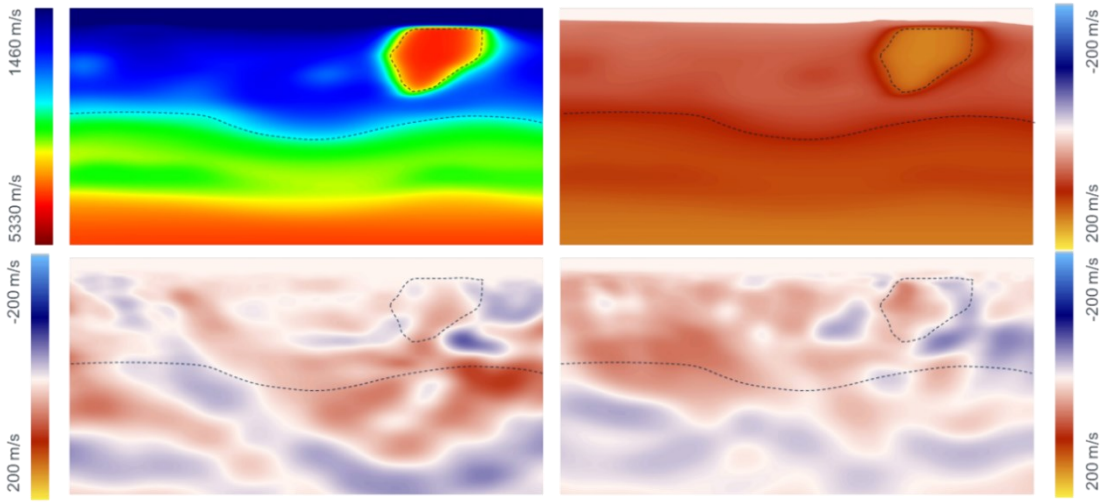

Figure 3 *Ultra-low frequency FWI results on data band passed by a zero-phase filter with corner frequencies 0.2, 0.5, 0.6 and 1.6 Hz. Top left: towed streamer WAZ derived velocity model. Top right: 3% perturbation of that model. Bottom left: FWI velocity update based on deblended data. Bottom right: FWI velocity update based on decoded data. Dashed lines are auxiliary lines for ease of interpretation. Vertical axes span roughly 12 km, horizontal axes span roughly 17 km.*

Conclusions and Outlook

In this small-scale test, hexa-source encoded Apparition shooting at 1,500 psi led to better SNR in the data domain and a better velocity update for low frequency FWI than dithered quad source data at 2,000 psi, while being on par for RTM imaging. This opens up the road for more efficient and higher quality nodal surveys for Exploration.

Acknowledgements

The authors would like to thank TGS management for approval to publish these results and Milos Cvetkovic for review of the document.

References

Abma, R., and M. S. Foster [2020] *Simultaneous source seismic acquisition*: SEG.

Amundsen, L., Andersson, F., van Manen, D-J., Robertsson, J.O.A. and Eggenberger, K. [2018] *Multisource encoding and decoding using the signal apparition technique*, Geophysics, 47.

Andersson, F., Robertsson, J. O. A., van Manen, D. J., Wittsten, J., Eggenberger, K., and Amundsen, L. [2017] *Express Letters: Flawless diamond separation in simultaneous source acquisition by seismic apparition*: Geophysical Journal International, 209 (3), 1735-1739.

Baeten, G., Hunt, K., Kuvshinov, B., Macintyre, H., McDonald, M., Nolan, B., Rambaran, V., and ten Kroode, F. [2021] *Cheaper and Better Long Offset Nodal Surveys Based on Low-Frequency Enhanced Sources*, EAGE Extended Abstracts.

JafarGandomi, A., Holland, S. and Grion, S. [2021] *Adaptive de-blending of dithered simultaneous sources*, First Break, 39, 37-44.

Kumar, A., Hampson, G., Vice, N., and Thompson, T. [2020] *An inversion-based deblending solution*, SEG Expanded Abstracts, 2769-2773.

Udengaard, C,, Brookes, D., and Flores, H. [2023] *Gemini: a fully operational broadband source for model building and imaging*, IMAGE Expanded Abstracts.